Talanta 233 (2021) 122594

Contents lists available at ScienceDirect

Talanta

journal homepage: www.elsevier.com/locate/talanta

Copper sulfide nanoclusters with multi-enzyme-like activities and its application in acid phosphatase sensing based on enzymatic cascade reaction

Yujiao Zhang [a,1], Shuqing Yang [a,1], Jin Wang [b], Yuanyuan Cai [c], Lingxi Niu [a], Xuan Liu [a], Chongyang Liu [c], Huan Qi [d,**], Aihua Liu [a,c,*]

[a] Institute for Chemical Biology & Biosensing, College of Life Sciences, Qingdao University, 308 Ningxia Road, Qingdao, 266071, China
[b] Qingdao Institute for Food and Drug Control, 7 Longde Road, Qingdao, 266073, China
[c] School of Pharmacy, Medical College, Qingdao University, 308 Ningxia Road, Qingdao, 266071, China
[d] Shanghai Center for Systems Biomedicine, Key Laboratory of Systems Biomedicine (Ministry of Education), Shanghai Jiao Tong University, Shanghai, 200240, China

ARTICLE INFO

Keywords:
CuS nanoclusters
Peroxidase-like
Catalase-like
SOD-like
AAO-like
Acid phosphatase sensor

ABSTRACT

Nanozymes are artificial enzymes, which can substitute natural enzymes for wide range of catalysis-based applications. However, it is challenging to explore novel mimic enzymes or multi-enzyme mimics. Herein we report the facile preparation of uniform CuS nanoclusters (NCs), which possessed outstanding tetra-enzyme mimetic catalytic activities, including peroxidase (POD)-mimics, catalase (CAT)-mimics, ascorbic acid oxidase (AAO)-mimics and superoxide dismutase (SOD)-mimics. The catalytic mechanism of POD-like was coming from the oxygen vacancies of CuS. Furthermore, the steady-state kinetics of POD-, CAT- and AAO mimics of CuS NCs were systematically explored. On basis of the enzymatic cascade reaction that acid phosphatase (ACP) involved in a weak acidic environment, in the presence of *O*-phenylenediamine, quinoxaline fluorescent substance will be generated. Thus, a fluorescent biosensor platform was proposed for detection of ACP with the linear range of 0.05–25 U L^{-1} and limit of detection of 0.01 U L^{-1}. The as-proposed method was applicable to real serum sample detection accurately and reproducibly. Considering the simple preparation, good stability, excellent multi-enzyme activities and controllable experimental operation, CuS NCs would provide a basis for expanding to other biocatalytic and biomedical applications.

1. Introduction

Natural enzymes have good catalytic activity but experience stability issue and high cost due to their complicated processing [1–4]. As a result, more and more nanostructures based enzyme mimics have been developed to overcome shortcomings [5]. Compared with natural enzymes, nanostructured mimic enzymes have a series of advantages [6] such as controllable synthesis and resistance to harsh environments [7], which have been found a wide range of catalysis-based applications in biosensing [8–10], tumor therapy [11,12], biomimetic synthesis [13] and antibacterial [14]. At present, various enzymes-like such as oxidase-like, peroxidase (POD)-like [15], catalase (CAT)-like and superoxide dismutase (SOD)-like have been simulated [16]. With the advent of nanotechnology, artificial mimic enzymes [17] have been extensively studied, but most of them are single functional mimic enzymes and double functional mimic enzymes, for example, noble metal nanoparticles (NPs) including gold NPs and silver NPs demonstrating POD-like activity [18], while platinum NPs having both uric acid enzyme and POD-like activities [19], however, the synthesis is cost-expensive. To solve this issue, a large number of transition metal containing nanomaterials having enzyme activity are reported, such as Fe_2O_3 NPs [20], CeO_2 NPs [21], MnO_2 nanosheets [22,23], CuO NPs [24], $NiFe_2O_4$ nanorods (NRs) [25], CoO NPs [26], Co_3O_4 nanospheres [8,27] and MoO_3 NRs/C [10]. Obviously, to construct artificial enzymes with simple chemical synthesis by simulating the active center of natural enzymes becomes a powerful means to solve the inherent defects of

* Corresponding author. Institute for Chemical Biology & Biosensing, College of Life Sciences, Qingdao University, 308 Ningxia Road, Qingdao, 266071, China.
** Corresponding author.
E-mail addresses: qihuan@sjtu.edu.cn (H. Qi), liuah@qdu.edu.cn (A. Liu).
[1] These authors contributed equally to this work.

https://doi.org/10.1016/j.talanta.2021.122594
Received 24 March 2021; Received in revised form 3 June 2021; Accepted 5 June 2021
Available online 12 June 2021

natural enzymes. On the other hand, although many metal compound nanomaterials have been proved to have nano-enzyme properties [28,29], but the dispersion of these nanostructures in aqueous media has been challenged when applied in practice [30]. Therefore, it is very important to find a method to ensure the good dispersion and stability of nanoparticles in water [31]. More importantly, it is challenging to explore multi-enzyme mimics for real applications.

Copper-based nanomaterials have attracted much interests in many fields including biosensing [32,33], photothermal therapy and killing bacteria [34–38] due to their superb photothermal conversion properties and low toxicity. Actually, copper nanostructures can be used as fluorescent probes for sensing and biological imaging [24,39,40]. Additionally, Cu-based nanomaterials have potential to be promising alternative enzyme mimetics [41,42]. Among them, copper sulfide (CuS) and copper oxide (CuO) have attracted a lot of interest due to their simple synthesis process [43], excellent catalytic performance and low toxicity [44–46]. Due to their biocompatibility and high chemical stability, CuS has been developed rapidly, and can be used in biosensors [47,48] and biomedical fields [49–52] based on its single nanozyme or dual enzyme activity or photocatalysis. Although CuS nanoparticles were reported to exhibit single POD-like activity, however, they were prepared under harsh conditions such as high temperature or non-aqueous phase, especially, their sizes are usually large and not uniform [53–58]. Therefore, it is a challenge to prepare CuS nanoparticles based multiple enzyme mimics with small and uniform size under mild conditions.

Herein, we report that CuS nanoclusters (NCs) possess excellent multi-enzyme-like catalytic activities: POD-like, SOD-like, ascorbic acid oxidase (AAO)-like and CAT-like activity. Further, the steady-state catalytic kinetics of CuS NCs were extensively investigated. Finally, a novel fluorescent biosensor was constructed for acid phosphatase (ACP), based on the enzymatic cascade reaction that in a weak acidic environment, ACP can catalyze sodium ascorbate phosphate (AAP) to produce ascorbic acid (AA), which is subsequently oxidized catalytically by AAO-like of CuS to dehydroascorbic acid, reacting with *O*-phenylenediamine to produce fluorescent agent quinoxaline. The as-proposed method was applicable to real human serum sample detection accurately and reproducibly.

2. Experimental section

2.1. Chemicals and materials

Bovine serum albumin (BSA), *O*-phenylenediamine (OPDA), copper chloride ($CuCl_2$), trisodium citrate dihydrate and sodium sulfide nonahydrate ($Na_2S{\cdot}9H_2O$) was bought from J&K Scientific Ltd. Methionine, hydrogen peroxide (H_2O_2, 30 wt%), nitro blue tetrazolium (NBT), riboflavin, p-benzoquinone (BQ), ethylenediaminetetraacetic acid salt (EDTA), methyl orange (MO), sodium azide (NaN_3), ammonium oxalate ($(NH_4)_2C_2O_4$), isopropanol (IPA), ACP, AAP and AA were obtained from Sino pharm Chemical Co,. Ltd. (Shanghai, China). Alkaline phosphatase (ALP), alcohol dehydrogenase (ADH), gluathione reductase (GR) was purchased from Solarbio Science & Technology Co., Ltd (Bejing, China). 3,3′,5,5′-tetramethylbenzidine (TMB) was purchased from TCI Development Co., Ltd (Shanghai, China).

2.2. Instruments

Transmission electron microscopic (TEM) images were observed on an F20 S-TWIN instrument (FEI, USA). The absorption spectra and absorbance were measured by a U-2910 spectrophotometer (Hitachi, Japan) and a SPARK 10M microplate reader (Tecan, Switzerland). Fluorescent spectra were monitored with an F-7000 fluorescence spectrophotometer (Hitachi, Japan).

2.3. Preparation of CuS NCs

To prepare CuS NCs, sodium citrate solution (5.0 mL, 8 mM) was added to $CuCl_2$ solution (5.0 mL, 8.0 mM), which was stirred for 5 min. Then, Na_2S solution (5.0 mL, 16.0 mM) was dropwise syringed into above solution under vigorous stirring for 15 min at 37 °C. Afterwards, BSA solution (5.0 mL, 50 mg mL^{-1}) was added to the above mixture solution and incubated at 37 °C for 8 h. Finally, the solution was dialyzed against water for 24 h. The thus-yielded CuS was stored in darkness at 4 °C.

2.4. CuS with multiple enzyme activities

2.4.1. Discovery of CuS POD-like activity

To research the POD-like activity of CuS NCs, CuS (0.4 mM), H_2O_2 (10 mM) and TMB (1.0 mM) were added separately to 0.1 M acetate buffer (pH 3) for 30 min at room temperature. The experimental group and the system without CuS or H_2O_2 were used as the control group. The absorbance of the solution at 652 nm was monitored by a microplate reader.

2.4.1.1. Study on the mechanism of POD-like. To study the catalytic mechanism of POD mimetics of CuS NCs, EDTA (3.0 mM), IPA (10 mM) and NaN_3 (50 mM) were added respectively to a 0.1 M acetate buffer (pH4.5) containing H_2O_2 (10 mM) and CuS NCs (0.67 mM). Finally, TMB was added to the system and incubated for 30 min in a water bath at 40 °C. A microplate reader was used to detect the absorbance of the solution at 652 nm. BQ (1.0 mM) was syringed into a 0.1M acetate buffer (pH 4.5) mixed with MO (2.0 μM), CuS (0.67 mM) and H_2O_2 (10 mM). The mixture solution was illuminated 70 min under a fluorescent lamp. Finally, a microplate reader was used to detect the absorbance of the solution at 463 nm.

2.4.2. Discovery of CuS mimic CAT activity

To investigate whether CuS has CAT-like activity, CuS (0.4 mM) and H_2O_2 (20 mM) were syringed to 0.1 M Tris-HCl buffer (pH 9.0) and incubated at 25 °C for 30 min. The spectra of the mixed solution was monitored by spectrophotometer.

2.4.3. Discovery of CuS mimic SOD activity

To investigate whether CuS has SOD-like activity was detected by NBT reduction method. Riboflavin and methionine can produce superoxide anions, the latter can reduce NBT to generate blue armor hydrazine with a characteristic peak at 560 nm. The SOD-like activity could remove superoxide anions and inhibit the reduction process, thus the decrease of absorption peak at 560 nm was observed. In detail, CuS (0.67 mM), riboflavin (2 μM), methionine (13 mM), NBT (75 μM) and EDTA (10 μM) were added to a 100 mM phosphate buffer (PBS, pH7.4) and incubated for 15 min in light and darkness respectively, and the absorbance of the solution at 560 nm was detected.

2.4.4. Discovery of CuS AAO activity

In order to investigate whether CuS has AAO-like activity, CuS (0.2 mM) and AA (1.0 mM) were added to 100 mM PBS (pH 6) and reacted for 2 min at 25 °C. The absorbance of the mixed solution at the wavelength of 265 nm was detected by spectrophotometer.

2.5. Analysis of catalytic kinetic parameters

Kinetic parameters of POD activity of CuS were studied. The whole reaction system was performed in 100 mM acetic acid buffer (pH 4.5). Under other optimization conditions, the absorbance of the reaction system at wavelength of 652 nm was determined by fixing the concentration of H_2O_2 (20 μM) while changing the concentration of TMB, or fixing the concentration of TMB (2.0 mM) while changing the

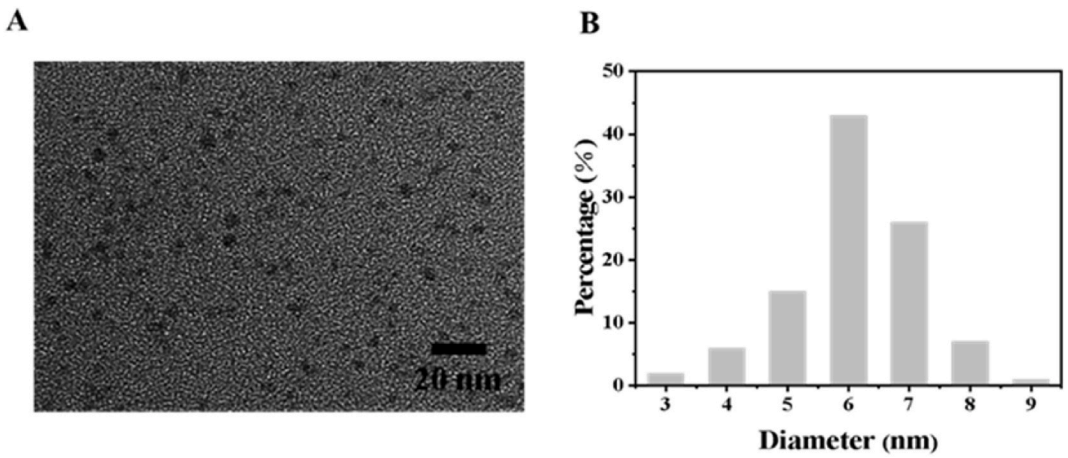

Fig. 1. (A) TEM images and (B) size distribution of the as-prepared CuS NPs.

concentration of H_2O_2.

Kinetic parameters of CAT-like activity of CuS were studied. The whole reaction system was performed in 100 mM Tris-HCl buffer (pH 9). Under optimization conditions, the absorbance of the reaction system at wavelength of 240 nm was determined with varying H_2O_2 concentration.

Kinetic parameters of AAO-like simulated by CuS were studied. The whole reaction system was carried out in phosphate buffer (100 mM, pH 6). Under the optimized conditions, the absorbance of the reaction system at 265 nm was determined with varying AA concentration.

According to the Lineweaver Burk equation, $\mathbf{v} = \frac{\mathbf{V_{max}[S]}}{\mathbf{K_m}+\mathbf{[S]}}$.

where V_{max}, V, K_m, and [S] is defined as maximum reaction rate, initial reaction rate, Michaelis-Menten constant and substrate concentration, separately.

2.6. ACP sensing by AAO-like activity of CuS

200 μL reaction solution with AAP (1.0 mM), different ACP concentrations and acetate buffer (100 mM, pH 5) was incubated at 37 °C for 15 min. Then, 100 μL of the above reaction solution was added to the phosphate buffer (pH 6) containing OPD (1.0 mM) and CuS (0.4 mM) and reacted for 4 min. The fluorescent spectra were measured.

3. Results and discussion

3.1. Preparation and characterization of CuS NCs

We used BSA as a template to synthesize CuS NCs under mild condition. That is, it is performed in aqueous solution at room temperature. In a typical synthesis procedure, the $CuCl_2$ solution became dark blue with the addition of sodium citrate under stirring. Further, the solution became dark brownish with the addition of Na_2S solution. Finally, BSA was added to stabilize the nanostructures considering that BSA is a water-soluble protein. The obtained nanoparticles were water-soluble, which were uniformly dispersed from TEM images (Fig. 1A) with the size of 6.0 ± 0.4 nm (Fig. 1B), typical of nanoclusters.

3.2. Multiple enzyme activities of CuS NCs

3.2.1. POD mimetics

3.2.1.1. Characterization of POD mimetics. The POD-like mimetics of CuS NCs was studied based on the typical color reaction produced by TMB with H_2O_2 and POD. The reaction system without CuS or H_2O_2 had tiny absorption peak at 652 nm, while CuS/TMB/H_2O_2 system exhibited remarkable absorption peak at 652 nm. These results indicate that CuS has POD-like catalytic activity (Fig. 2). Further we optimized the important parameters including solution, pH, temperature, material dosage, and TMB concentration that affect the catalytic activity of CuS. As shown in Fig. S1, the maximum POD-like activity of CuS NCs was obtained at pH 4.5 and 45 °C, respectively.

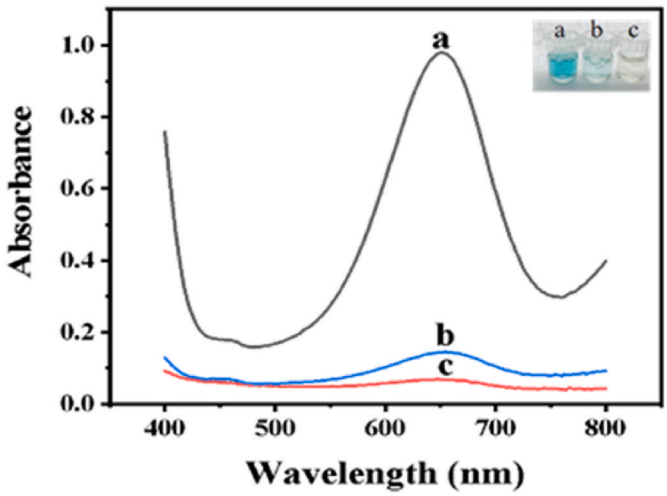

Fig. 2. The visible spectrum of (a) CuS (0.4 mM)/TMB (1.0 mM)/H_2O_2 (10 mM), (b) CuS (0.4 mM)/H_2O_2 (10 mM), (c) TMB (1.0 mM)/H_2O_2 (10 mM). The above systems in an acetate buffer of (pH 3) at 30 °C reaction for 30 min.

3.2.1.2. Study on the catalytic mechanism of mimic POD activity of CuS. We found that when BQ (a scavenger for $O_2^{\bullet-}$), IPA (a scavenger for •OH) and NaN_3 (a scavenger for $^1O_2$) [59,60] were separately added into CuS/TMB/H_2O_2 system, the absorbance value of above system did not decrease significantly (Fig. 3A,B,C). These results indicate that $O_2^{\bullet-}$, •OH and $^1O_2$ are not the major active substances in the reaction solution [61]. However, when EDTA was added, the absorbance at 652 nm of the reaction system was significantly reduced (Fig. 3D). Therefore, we assume that the mechanism of POD-like of CuS NCs was owing to oxygen vacancies [62].

3.2.2. CAT mimetics activity of CuS

The CAT-like activity of CuS was explored based on the decrease in the absorbance of H_2O_2 at a wavelength of 240 nm. CuS (0.4 mM) was added into H_2O_2 (20 mM) and reacted at room temperature. After 45 min, a decrease in the absorbance at 240 nm was detected (Fig. 4). The CAT-like activity of CuS NCs was further optimized, and the results

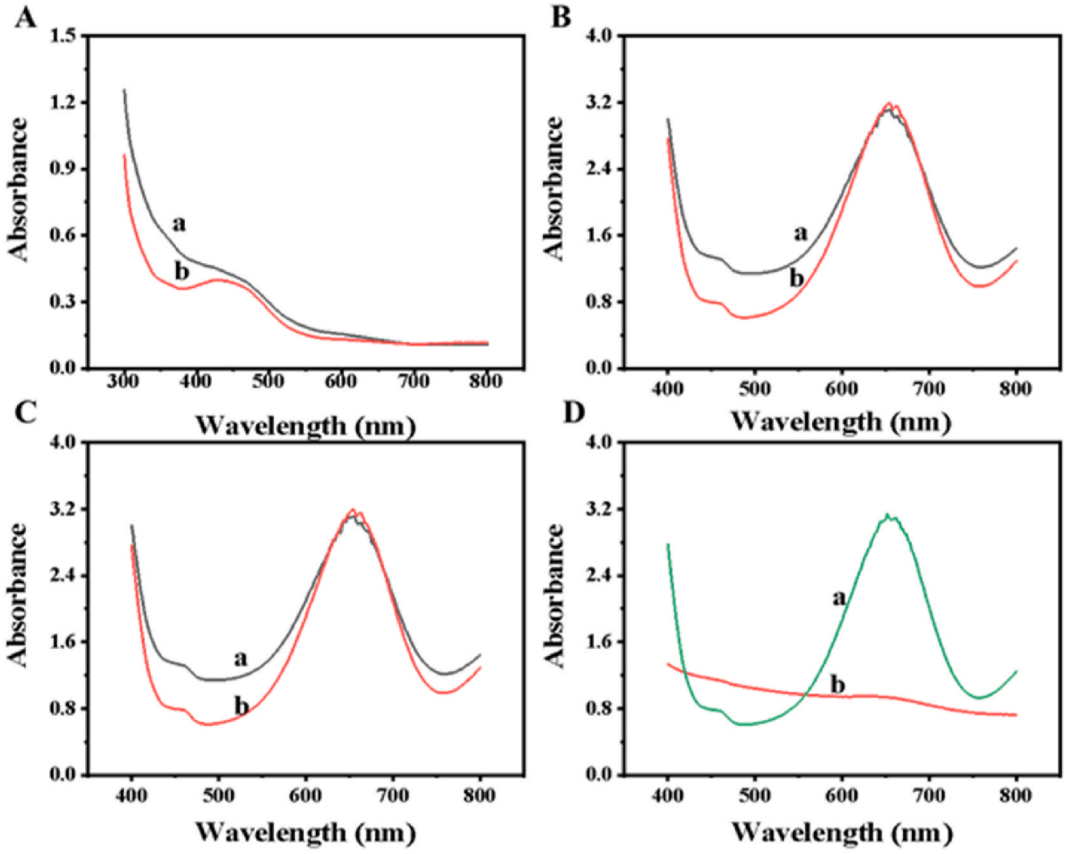

Fig. 3. Effect of scavengers. (**A**) 1.0 mM BQ as $O_2^{\bullet-}$ scavengers (MO as color agent). (**B**) 10 mM IPA as •OH scavengers. (**C**) 3.0 mM NaN_3 as $^1O_2$ scavengers. (**D**) 50 mM EDTA as oxygen vacancies scavengers. In above cases, CuS (0.67 mM), H_2O_2 (10 mM) and TMB (2.0 mM) were mixed into acetate buffer (pH 4.5) including various scavengers at 40 °C for 30 min with (a) or without scavengers (b). (For interpretation of the references to color in this figure legend, the reader is referred to the Web version of this article.)

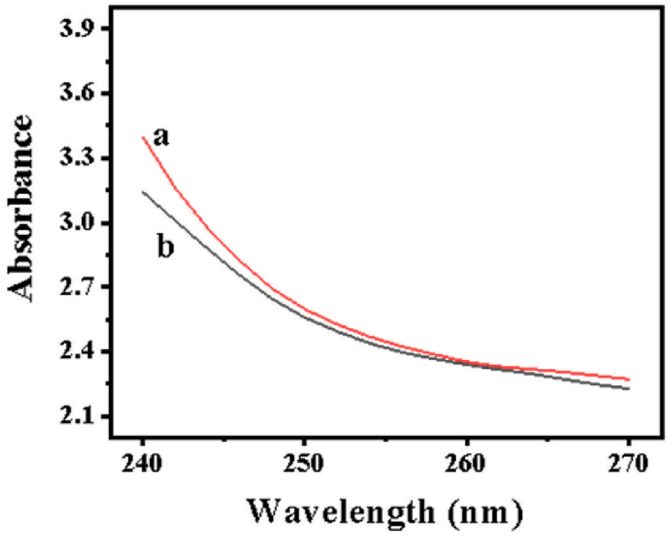

Fig. 4. The UV spectra of CuS (0.4 mM)/H_2O_2 (20 mM) system (pH 9) at different time. (a) 0 min, (b) 45 min.

showed CuS exert the best CAT activity when pH was 9 (Fig. S2A). As mentioned above, the optimal POD activity of CuS NCs was pH 4.5 and the activity decreased within the pH range of 4.5–10. By contrast, CuS NCs show excellent CAT activity within the pH range of 4.5–10 and the best CAT activity at pH 9, indicating that the POD activity of CuS does not interfere with the CAT activity. Taking into account the temperature and CuS dosage has an effect on its CAT-like activity, we further optimized the reaction conditions. As the temperature increases, the relative activity of CAT activit gradually increased and a peak reached at 60 °C (Fig. S2B). When the CuS NCs concentration increases, the absorbance at 240 nm gradually increases and a plateau reaches after 0.25 mM (Fig. S2C), which indicates that the CAT-like activity of CuS will increase with the increase of the concentration of the CuS.

3.2.3. *SOD-like activity of CuS NCs*

We used the classic NBT colorimetric method to testify whether CuS NCs has SOD mimcking activity. Compared with the system without CuS, the absorbance at 560 nm of the system containing CuS decreased significantly (Fig. 5A), which indicated that CuS had SOD-like activity and inhibited the reduction of NBT. With the increase of concentration, the absorption value at 560 nm decreases (Fig. 5B). Then, with the concentration of CuS as a variable, the inhibition rate curve was drawn based on the following formula: Inhibition rate $=(A_{blank}\text{-}A_{sample})/(A_{blank}) \times 100\%$. Here A_{blank}, A_{sample} denotes the absorbance at 560 nm of blank solution and CuS NCs, respectively. It can be concluded that when the concentration of CuS is 0.67 mM, the inhibition rate of the reduction process of NBT reaches the maximum (Fig. 5C).

3.2.4. *AAO-like e activity of CuS*

The AAO-like activity of CuS was detected based on the decrease in absorbance of AA at the maximum absorption wavelength of 265 nm. CuS (0.2 mM) was added to 1.0 mM AA and reacted for 3 min at room temperature. To detect the decrease in the absorbance at 265 nm, we recorded the spectra every 30 s (Fig. 6). Under the catalysis of CuS, as

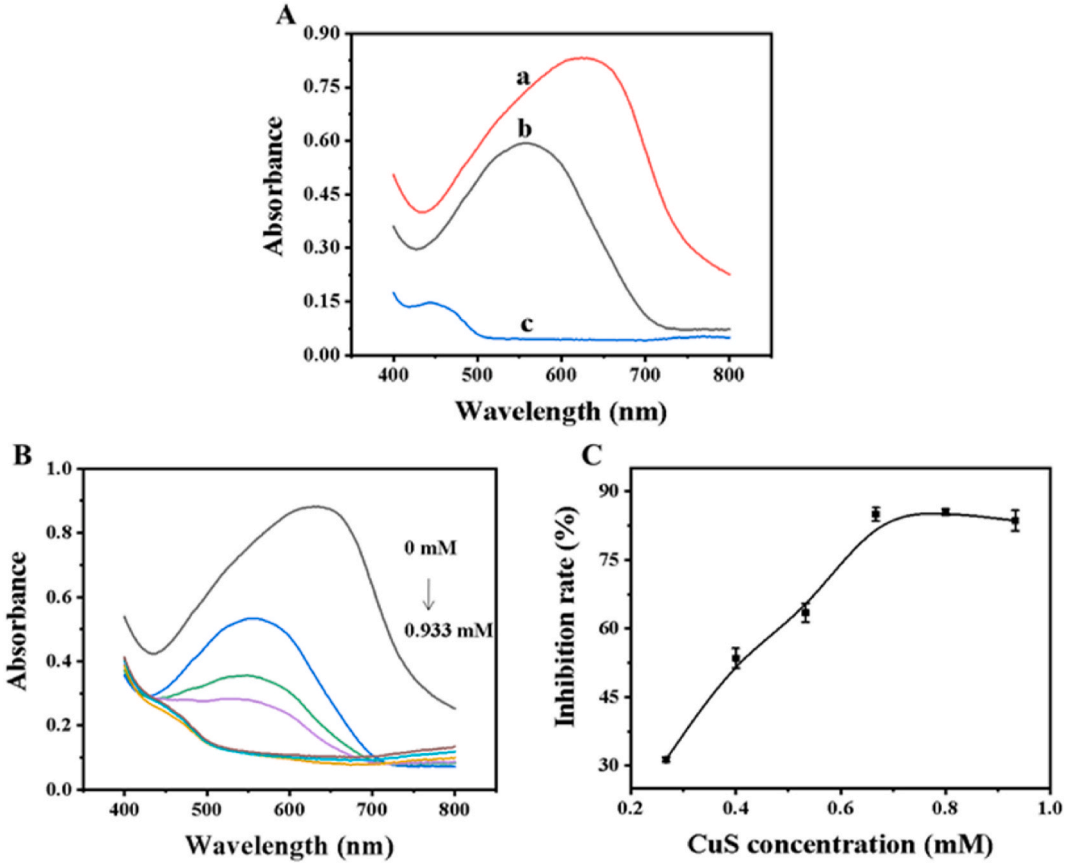

Fig. 5. (**A**) The visible spectra of the mixture solution of NBT/riboflavin/methionine/EDTA under varying conditions. (a) without CuS, (b) CuS (0.67 mM) with illumination. (c) CuS (0.67 mM) without illumination. Incubation conditions: in buffer pH 7.4, at temperature of 25 °C, reaction time of 15 min. (**B**) The visible absorption spectra of systems in which different concentration of CuS were added. (**C**) The inhibition rate of CuS to NBT changing with CuS concentration. Incubation conditions, in buffer pH 7.4, at temperature of 25 °C, reaction time was 15 min.

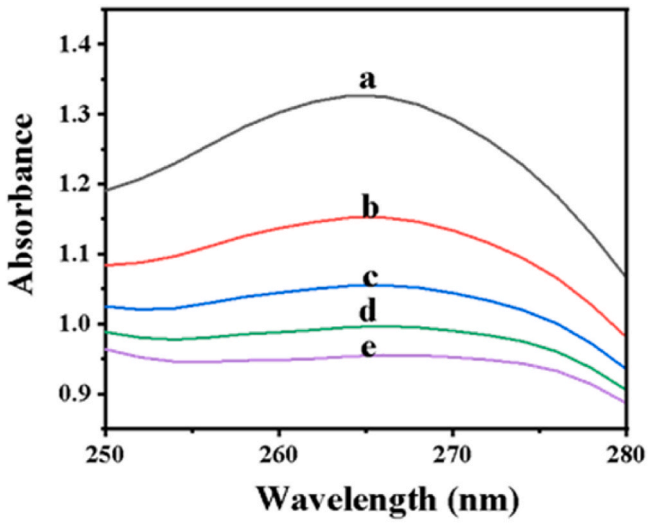

Fig. 6. Evolution of UV spectra for 0.2 mM CuS with 1.0 mM AA in pH 6 buffer at different reaction time: (a) 0 s, (b) 30 s, (c) 60 s, (d) 90 s, (e) 120 s.

time went on, the characteristic absorption peak of AA at 265 nm gradually became flat, indicative of CuS having AAO-like activity. We further explored the conditions that affect CuS catalyzed AA oxidation (Fig. S3), where the ordinate is $(A_0\text{-}A)/A_0$, A_0 and A are the absorbance values of the reaction system at 265 nm at the beginning of the reaction and after 3 min of reaction, respectively. Furthermore, by changing the pH of the buffer in the reaction system, CuS catalyzed AA oxidation exhibited the best activity at pH 6 (Fig. S3A). With the passage of reaction time, the reaction of CuS catalyzed AA oxidation was completed at 3 min (Fig. S3B). Considering that temperature and CuS concentration will also affect the progress of the entire reaction system, we have subsequently optimized the temperature to be 35 °C (Fig. S3C) and CuS concentration (Fig. S3D).

3.3. Catalytic kinetic inquiry of POD-like, CAT-like and AAO-like of CuS

The catalytic kinetic parameters of CuS POD-like activity were detected by fixing the concentration of H_2O_2 or TMB while changing the concentration of TMB or H_2O_2, and plotted double reciprocal linear Burk curve (Fig. S4). For TMB and H_2O_2, the linear regression equations are $y = 5.45x + 13.33$ ($R^2 = 0.999$) and $y = 7.39x + 18.19$ ($R^2 = 0.999$), respectively, the K_m value with CuS NCs is calculated to be 0.409 mM (TMB) and 0.406 mM (H_2O_2). Compared with the reported mimic enzymes with POD-like activity (Table S1), CuS has a stronger affinity for the substrate for catalysis. The V_{max} is calculated to be 0.0632 μM s^{-1} (TMB) and 0.0549 μM s^{-1} (H_2O_2).

In the same way, the catalytic kinetic process and catalytic activity of CAT-like mimics for CuS NCs were investigated. Within a certain concentration range, the kinetics of the reaction system was studied with H_2O_2 as the substrate, and the double reciprocal line was drawn with the linear regression equation of $y = 1.309x + 0.239$ ($R^2 = 0.995$) (Fig. S5). The main kinetic parameters such as K_m and V_{max} are calculated to be 5.47 mM and 4.18 μM s^{-1}, respectively. Compared with other catalysts in Table S2, CuS NCs exhibited good affinity for H_2O_2.

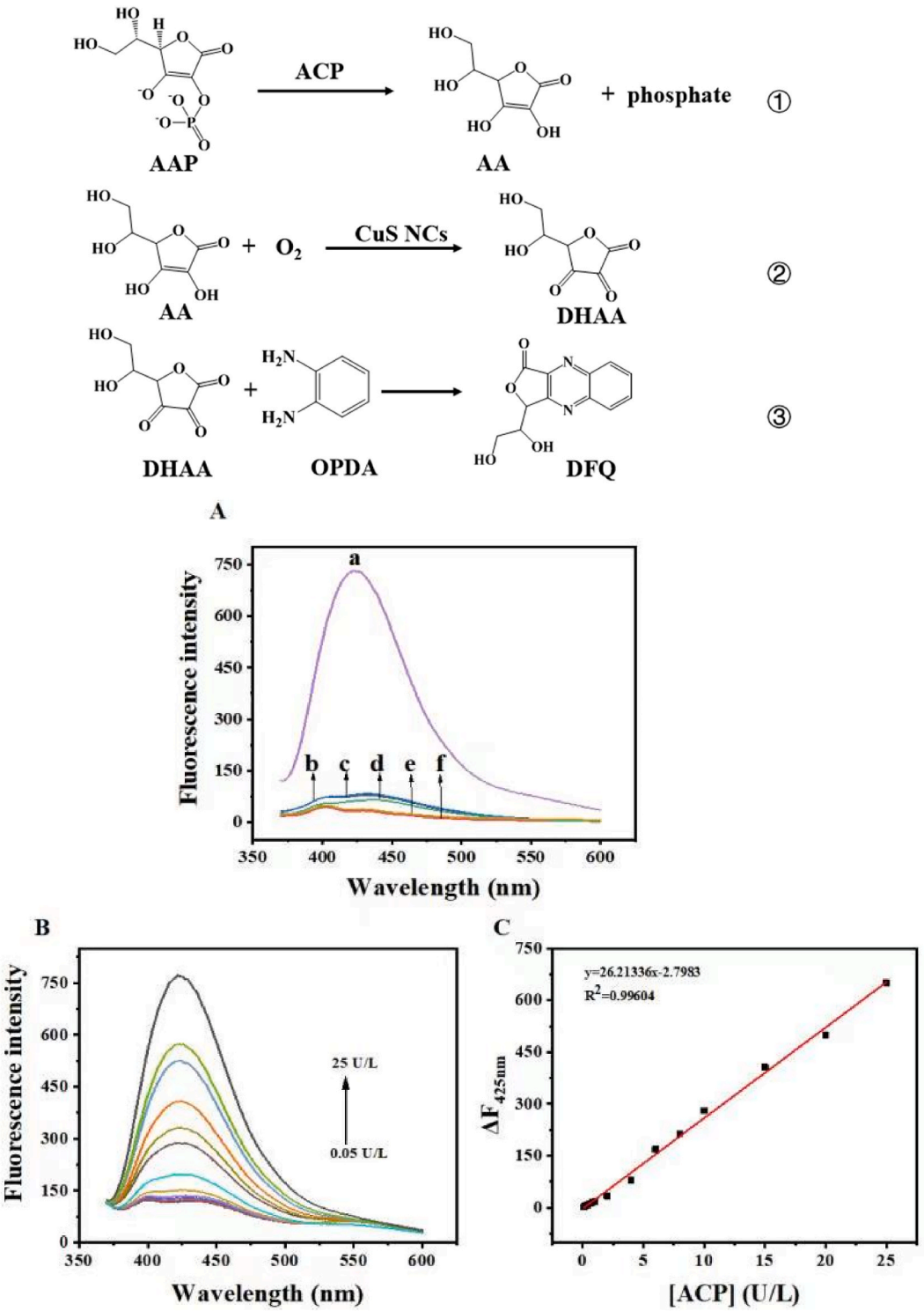

Fig. 7. (A) Fluorescence spectra of OPDA/AAP/ACP/CuS NCs (a) OPDA/CuS NCs (b) OPDA/AAP/CuS NCs (c) CuS NCs (d) OPDA (e) and OPDA/AAP (f). (B) The fluorescence spectra of the system with different concentrations of ACP. (C) Calibration curve for ACP determination. The reaction condition: AAP (1.0 mM) and ACP in the acetate buffer (pH 5) incubation for 15 min at 37 °C. Then, 100 μL of the above solution was shifted to the phoshpate buffer (pH 6) containing CuS (0.4 mM) and OPD (1.0 mM) and reacted for 4 min. Excitation wavelength, 350 nm.

In order to explore the catalytic kinetics of CuS AAO-like mimics and catalytic activity, we used AA as the substrate to study the steady-state kinetics. On this basis, the double reciprocal Burk curve (Fig. S6) can be drawn with the linear regression equation of $y = 0.0248x + 0.226$ ($R^2 = 0.999$). The K_m and V_{max} are calculated to be 0.087 mM and 4.41 μM s^{-1}, respectively. That is, CuS NCs exhibited almost the same K_m with natural AAO in Table S3, indicating that CuS NCs had the similar affinity for the substrate with AAO.

3.4. Fluorimetric ACP sensor based on enzymatic cascade reaction

The detection of ACP can be used as an auxiliary means of diagnosing prostate cancer. As shown in the enzymatic cascade reaction (Eqs1-2), ACP can catalyze the hydrolysis of AAP in an acidic environment to

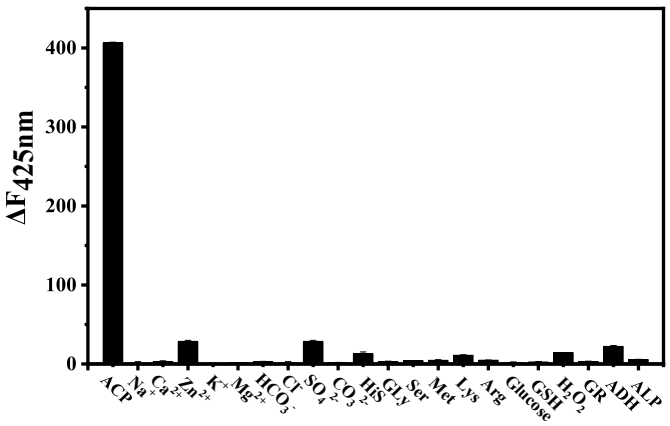

Fig. 8. Selectivity test of ACP detection. The concentration of ACP, 15 U L^{-1}; GSH, 20 μM; H_2O_2, 0.2 mM; ion species, 20 mM, GR, 70 U L^{-1}; ADH, 56 U L^{-1}; ALP, 120 U L^{-1}; other interfering substances, 5 mM. ACP (15 U L^{-1}) in the presence of testing interference species were added to the acetate buffer, the mixed solution was incubated at 37 °C for 15 min. 100 μL of the above solution was transferred into the phoshpate buffer (pH 6) containing CuS (0.4 mM) and OPDA (1.0 mM), and detected fluorescence @ 425 nm after 4 min incubation.

Table 1
Detection of ACP in human serum samples.

Sample	Known conc. (U/L)	Spiked (U/L)	Detected conc. (U/L)	Recovery (%)	RSD (n = 3)
#1	12.7	0	12.6 ± 0.3	–	2.4%
		3.0	15.8 ± 0.4	106.7	2.5%
		6.0	18.8 ± 0.4	103.4	2.1%
#2	19.3	0	19.5 ± 0.5	–	2.6%
		2.0	21.6 ± 0.4	105.0	1.9%
		4.0	23.5 ± 0.5	100.0	2.1%

produce phosphate and AA, of which AA can be further oxidized to dehydroascorbic acid (DHAA) catalyzed by AAO mimics of CuS. Finally, DHAA can react with OPD to produce quinoxaline fluorescent agent (Eq.3). OPDA/AAP/ACP/CuS NCs system exhibited typical fluorescent peak at 425 nm (Fig. 7A). As the concentration of ACP increased, the fluorescence intensity of the reaction system became stronger and stronger (Fig. 7B). Fig. 7C reflects the changes in the fluorescence intensity of the system varying with ACP concentrations at 425 nm. To fit linearly, it can be seen that the fluorescence intensity @ 425 nm linearly increases with the ACP concentration within 0.05–25 U L^{-1} (Fig. 7C). The limit of detection (LOD) is calculated as 0.01 U L^{-1} (S/N = 3). As summarized in Table S4, for comparison of different methods for the detection of ACP, our proposed sensor shows good analytical performance regarding linear range and LOD, which contributed from CuS NCs' excellent AAO mimics activity and the enzymatic cascade reaction.

3.4.1. Selective experiment of CuS detecting ACP

The selectivity of the ACP method was evaluated by comparing the response of some potential interferences including glucose, various ions, amino acids and antioxidants as control. Then a histogram was drawn according to the changes in fluorescence intensity. For other test species, the fluorescence intensity is significantly weak, indicating that the CuS/AAP system has good selectivity for ACP (Fig. 8).

3.4.2. ACP detection in actual sample

In order to verify the feasibility of CuS in detecting ACP in actual samples, we obtained human serum samples containing different concentrations of ACP from local hospital. To remove possible matrix effects, standard addition method was used to detect actual samples. The ACP content in the serums were calculated. As shown in Table 1, the results of all samples measured by our method are in good agreement with clinical data, and the relative standard deviation (RSD) is within 3.0%.

3.5. Stability and repeatability of mimic enzyme

The stability and repeatability of mimic enzymes are very important in practical catalysis-related applications. The POD-like and AAO-like activity of CuS was evaluated weekly. After being placed at room temperature for 21 days, the relative activity of the POD mimics and AAO mimics of CuS NCs from three different batches can be maintained above 80% (Fig. 9), suggesting their good repeatability and stability.

4. Conclusions

In summary, CuS NCs prepared by using BSA as stabilizer had good dispersity in water media, which exhibited outstanding multiple enzyme catalytic activities, including POD mimics, CAT mimics, SOD mimics and AAO mimic. The steady-state catalytic kinetics of the tetra-enzyme mimics of CuS NCs was further investigated. The catalytic mechanism of CuS NCs imitated POD-like activity was oxygen vacancy dependent. Finally, based on enzymatic cascade reaction, a fluorescent biosensor platform was constructed to detect ACP sensitively and selectively. We believe that CuS NCs have broad application prospects in biosensors and biomedicine.

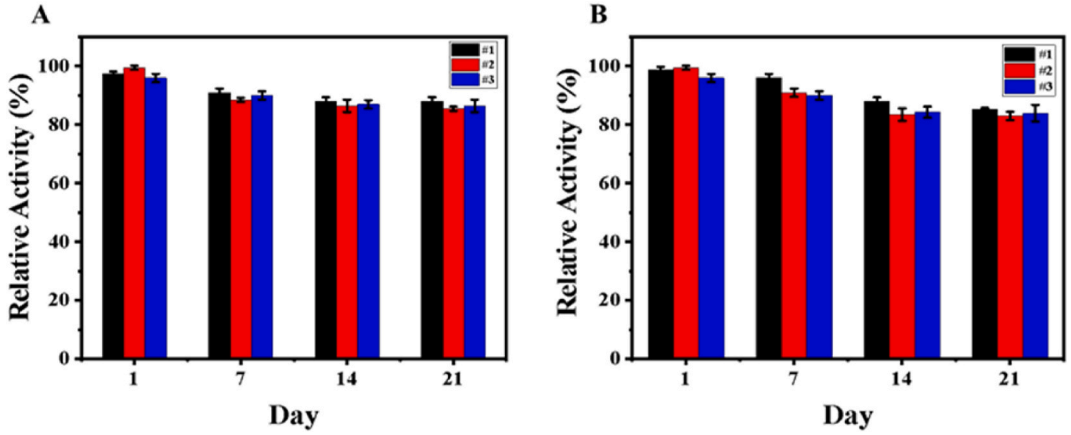

Fig. 9. Storage stability and repeatability of POD mimics (A) and AAO mimics (B) of different batches of CuS NCs in aqueous solution at room temperature.

Credit author statement

Yujiao Zhang: Methodology, Investigation and Writing - Original Draft. **Shuqing Yang:** Methodology, Investigation and Writing - Original Draft. **Jin Wang:** Investigation. **Yuanyuan Cai:** Investigation. **Lingxi Niu:** Investigation. **Xuan Liu:** Methodology. **Chongyang Liu**, Investigation. **Huan Qi:** Investigation and Writing - Review. **Aihua Liu:** Funding acquisition, Supervision, Conceptualization and Writing - Review & Editing.

Declaration of competing interest

The authors declare that they have no known competing financial interests or personal relationships that could have appeared to influence the work reported in this paper.

Acknowledgements

This work was financially supported by National Natural Science Foundation of China (Nos. 81673172, 51502036) and Major Program of Shandong Province Natural Science Foundation (ZR2018ZC0125).

Appendix A. Supplementary data

Supplementary data to this article can be found online at https://doi.org/10.1016/j.talanta.2021.122594.

References

[1] J. Wu, X. Wang, Q. Wang, Z. Lou, S. Li, Y. Zhu, L. Qin, H. Wei, Nanomaterials with enzyme-like characteristics (nanozymes): next-generation artificial enzymes (II), Chem. Soc. Rev. 48 (4) (2019) 1004–1076.
[2] L. Han, J. Shi, A. Liu, Novel biotemplated MnO_2 1D nanozyme with controllable peroxidase-like activity and unique catalytic mechanism and its application for glucose sensing, Sensor. Actuator. B Chem. 252 (2017) 919–926.
[3] S. Fan, B. Liang, X. Xiao, L. Bai, X. Tang, E. Lojou, S. Cosnier, A. Liu, Controllable display of sequential enzymes on yeast surface with enhanced biocatalytic activity toward efficient enzymatic biofuel cells, J. Am. Chem. Soc. 142 (6) (2020) 3222–3230.
[4] B. Liang, G. Wang, L. Yan, H. Ren, R. Feng, Z. Xiong, A. Liu, Functional cell surface displaying of acetylcholinesterase for spectrophotometric sensing organophosphate pesticide, Sensor. Actuator. B Chem. 279 (2019) 483–489.
[5] W. Shi, X. Zhang, S. He, Y. Huang, $CoFe_2O_4$ magnetic nanoparticles as a peroxidase mimic mediated chemiluminescence for hydrogen peroxide and glucose, Chem. Commun. (J. Chem. Soc. Sect. D) 47 (38) (2011) 10785.
[6] Y. Lin, J. Ren, X. Qu, Catalytically active nanomaterials: a promising candidate for artificial enzymes, Acc. Chem. Res. 47 (4) (2014) 1097–1105.
[7] J. Xie, X. Zhang, H. Wang, H. Zheng, Y. Huang, J. Xie, Analytical and environmental applications of nanoparticles as enzyme mimetics, Trac. Trends Anal. Chem. 39 (2012) 114–129.
[8] P. Liu, Y. Wang, L. Han, Y. Cai, H. Ren, T. Ma, X. Li, V.A. Petrenko, A. Liu, Colorimetric assay of bacterial pathogens based on Co_3O_4 magnetic nanozymes conjugated with specific fusion phage proteins and magnetophoretic chromatography, ACS Appl. Mater. Interfaces 12 (8) (2020) 9090–9097.
[9] H. Ren, X. Liu, L. Yan, Y. Cai, C. Liu, L. Zeng, A. Liu, Ocean green tide derived hierarchical porous carbon with bi-enzyme mimic activities and their application for sensitive colorimetric and fluorescent biosensing, Sensor. Actuator. B Chem. 312 (2020) 127979.
[10] H. Ren, L. Yan, M. Liu, Y. Wang, X. Liu, C. Liu, K. Liu, L. Zeng, A. Liu, Green tide biomass templated synthesis of molybdenum oxide nanorods supported on carbon as efficient nanozyme for sensitive glucose colorimetric assay, Sensor. Actuator. B Chem. 296 (2019) 126517.
[11] Y. Shen, H.D.A. Santos, E.C. Ximendes, J. Lifante, A. Sanz-Portilla, L. Monge, N. Fernández, I. Chaves-Coira, C. Jacinto, C.D.S. Brites, L.D. Carlos, A. Benayas, M. C. Iglesias-de la Cruz, D. Jaque, Ag_2S nanoheaters with multiparameter sensing for reliable thermal feedback during in vivo tumor therapy, Adv. Funct. Mater. 30 (2020) 2002730.
[12] D. Hu, Z. Sheng, S. Fang, Y. Wang, D. Gao, P. Zhang, P. Gong, Y. Ma, L. Cai, Folate receptor-targeting gold nanoclusters as fluorescence enzyme mimetic nanoprobes for tumor molecular colocalization diagnosis, Theranostics 4 (2) (2014) 142–153.
[13] G. Zan, Q. Wu, Biomimetic and bioinspired synthesis of nanomaterials/nanostructures, Adv. Mater. 28 (11) (2016) 2099–2147.
[14] A.U. Khan, Q. Yuan, Y. Wei, G.M. Khan, Z.U.H. Khan, S. Khan, F. Ali, K. Tahir, A. Ahmad, F.U. Khan, Photocatalytic and antibacterial response of biosynthesized gold nanoparticles, J. Photochem. Photobiol., B 162 (2016) 273–277.
[15] S. Singh, Nanomaterials exhibiting enzyme-like properties (nanozymes): current advances and future perspectives, Front. Chem. 7 (2019) 46.
[16] M. Liang, X. Yan, Nanozymes, From new concepts, mechanisms, and standards to applications, Acc. Chem. Res. 52 (8) (2019) 2190–2200.
[17] D.P. Cormode, L. Gao, H. Koo, Emerging biomedical applications of enzyme-like catalytic nanomaterials, Trends Biotechnol. 36 (1) (2018) 15–29.
[18] J. Li, W. Liu, X. Wu, X. Gao, Mechanism of pH-switchable peroxidase and catalase-like activities of gold, silver, platinum and palladium, Biomaterials 48 (2015) 37–44.
[19] Z. Wang, X. Yang, J. Yang, Y. Jiang, N. He, Peroxidase-like activity of mesoporous silica encapsulated Pt nanoparticle and its application in colorimetric immunoassay, Anal. Chim. Acta 862 (2015) 53–63.
[20] L. Song, C. Huang, W. Zhang, M. Ma, Z. Chen, N. Gu, Y. Zhang, Graphene oxide-based Fe_2O_3 hybrid enzyme mimetic with enhanced peroxidase and catalase-like activities, Colloids Surf., A 506 (2016) 747–755.
[21] M.M. Sozarukova, E.V. Proskurnina, A.E. Baranchikov, V.K. Ivanov, CeO_2 nanoparticles as free radical regulators in biological systems, Nanosystems: Physics, Chemistry, Mathematics 11 (3) (2020) 324–332.
[22] L. Han, P. Liu, H. Zhang, F. Li, A. Liu, Phage capsid protein-directed MnO_2 nanosheets with peroxidase-like activity for spectrometric biosensing and evaluation of antioxidant behaviour, Chem. Commun. 53 (37) (2017) 5216–5219.
[23] P. Liu, L. Han, F. Wang, X. Li, V.A. Petrenko, A. Liu, Sensitive colorimetric immunoassay of Vibrio parahaemolyticus based on specific nonapeptide probe screening from a phage display library conjugated with MnO2 nanosheets with peroxidase-like activity, Nanoscale 10 (6) (2018) 2825–2833.
[24] S.B. He, A.L. Hu, Q.Q. Zhuang, H.P. Peng, H.H. Deng, W. Chen, G.L. Hong, Ascorbate oxidase mimetic activity of copper(II) oxide nanoparticles, Chembiochem 21 (7) (2020) 978–984.
[25] H.Q. Alijani, S. Pourseyedi, M. Torkzadeh-Mahani, A. Seifalian, M. Khatami, Bimetallic nickel-ferrite nanorod particles: greener synthesis using rosemary and its biomedical efficiency, Artif. Cell. Nanomed. Biotechol. 48 (1) (2019) 242–251.
[26] Y. Guo, L. Yan, R. Zhang, H. Ren, A. Liu, CoO-supported ordered mesoporous carbon nanocomposite based nanozyme with peroxidase-like activity for colorimetric detection of glucose, Process Biochem. 81 (2019) 92–98.
[27] X. Liu, L. Yan, H. Ren, Y. Cai, C. Liu, L. Zeng, J. Guo, A. Liu, Facile synthesis of magnetic hierarchical flower-like Co_3O_4 spheres: mechanism, excellent tetra-enzyme mimics and their colorimetric biosensing applications, Biosens. Bioelectron. 165 (2020) 112342.
[28] Y. Li, S. Guo, Noble metal-based 1D and 2D electrocatalytic nanomaterials: recent progress, challenges and perspectives, Nano Today 28 (2019) 100774.
[29] X. Jiang, W. He, X. Zhang, Y. Wu, Q. Zhang, G. Cao, H. Zhang, J. Zheng, T. R. Croley, J.-J. Yin, Light-induced assembly of metal nanoparticles on ZnO enhances the generation of charge carriers, reactive oxygen species, and antibacterial activity, J. Phys. Chem. C 122 (51) (2018) 29414–29425.
[30] Y. Zhao, L. Jiang, Hollow micro/nanomaterials with multilevel interior structures, Adv. Mater. 21 (36) (2009) 3621–3638.
[31] Y. Liu, Y. Zheng, Z. Chen, Y. Qin, R. Guo, High-performance integrated enzyme cascade bioplatform based on protein-BiPt nanochain@graphene oxide hybrid guided one-pot self-assembly strategy, Small 15 (12) (2019) 1804987.
[32] Y. Liu, H. Jin, W. Zou, R. Guo, Protein-mediated sponge-like copper sulfide as an ingenious and efficient peroxidase mimic for colorimetric glucose sensing, RSC Adv. 10 (48) (2020) 28819–28826.
[33] A. Swaidan, P. Borthakur, P.K. Boruah, M.R. Das, A. Barras, S. Hamieh, J. Toufaily, T. Hamieh, S. Szunerits, R. Boukherroub, A facile preparation of CuS-BSA nanocomposite as enzyme mimics: application for selective and sensitive sensing of Cr(VI) ions, Sensor. Actuator. B Chem. 294 (2019) 253–262.
[34] W.F. Lai, W.T. Wong, A.L. Rogach, Development of copper nanoclusters for in vitro and in vivo theranostic applications, Adv. Mater. 32 (9) (2020), e1906872.
[35] J. Luo, C. Hein, F. Mucklich, M. Solioz, Killing of bacteria by copper, cadmium, and silver surfaces reveals relevant physicochemical parameters, Biointerphases 12 (2) (2017), 020301.
[36] X. Dai, Y. Zhao, Y. Yu, X. Chen, X. Wei, X. Zhang, C. Li, Single continuous near-infrared laser-triggered photodynamic and photothermal ablation of antibiotic-resistant bacteria using effective targeted copper sulfide nanoclusters, ACS Appl. Mater. Interfaces 9 (36) (2017) 30470–30479.
[37] C. Molteni, H.K. Abicht, M. Solioz, Killing of bacteria by copper surfaces involves dissolved copper, Appl. Environ. Microbiol. 76 (12) (2010) 4099–4101.
[38] A. Nain, Y.T. Tseng, S.C. Wei, A.P. Periasamy, C.C. Huang, F.G. Tseng, H.T. Chang, Capping 1,3-propanedithiol to boost the antibacterial activity of protein-templated copper nanoclusters, J. Hazard Mater. 389 (2020) 121821.
[39] K. Basu, S. Paul, R. Jana, A. Datta, A. Banerjee, Red-emitting copper nanoclusters: from bulk-scale synthesis to catalytic reduction, ACS Sustain. Chem. Eng. 7 (2) (2018) 1998–2007.
[40] X. Su, J. Liu, pH-guided self-assembly of copper nanoclusters with aggregation-induced emission, ACS Appl. Mater. Interfaces 9 (4) (2017) 3902–3910.
[41] C. Liu, Y. Cai, J. Wang, X. Liu, H. Ren, L. Yan, Y. Zhang, S. Yang, J. Guo, A. Liu, Facile preparation of homogeneous copper nanoclusters exhibiting excellent tetraenzyme mimetic activities for colorimetric glutathione sensing and fluorimetric ascorbic acid sensing, ACS Appl. Mater. Interfaces 12 (38) (2020) 42521–42530.
[42] Y. Cai, J. Wang, L. Niu, Y. Zhang, X. Liu, C. Liu, S. Yang, H. Qi, A. Liu, Selective colorimetric sensing sub-nanomolar Hg^{2+} based on its significantly enhancing peroxidase mimics of silver/copper nanoclusters, Analyst (2021), https://doi.org/10.1039/D1AN00512J in press.
[43] X. Niu, X. Xu, X. Li, J. Pan, F. Qiu, H. Zhao, M. Lan, Surface charge engineering of nanosized CuS via acidic amino acid modification enables high peroxidase-mimicking activity at neutral pH for one-pot detection of glucose, Chem. Commun. 54 (95) (2018) 13443–13446.

[44] Y. You, K. Qu, C. Shi, Z. Sun, Z. Huang, J. Li, M. Dong, Z. Guo, Binder-free CuS/ZnS/sodium alginate/rGO nanocomposite hydrogel electrodes for enhanced performance supercapacitors, Int. J. Biol. Macromol. 162 (2020) 310–319.
[45] Y. Cui, J. Zhang, G. Li, Y. Sun, G. Zhang, W. Zheng, Ionic liquid-assisted synthesis of rGO wrapped three-dimensional CuS ordered nanoerythrocytes with enhanced performance for asymmetric supercapacitors, Chem. Eng. J. 325 (2017) 424–432.
[46] Y. Bai, J. Liu, F. Feng, X. Yang, Synthesis of folic acid-mediated copper nanoclusters for the detection of sulfadiazine sodium, Colloids Surf., A 605 (2020) 125376.
[47] H. Jia, D. Yang, X. Han, J. Cai, H. Liu, W. He, Peroxidase-like activity of the Co_3O_4 nanoparticles used for biodetection and evaluation of antioxidant behavior, Nanoscale 8 (11) (2016) 5938–5945.
[48] L. Zhang, L. Han, P. Hu, L. Wang, S. Dong, TiO_2 nanotube arrays: intrinsic peroxidase mimetics, Chem. Commun. 49 (89) (2013) 10480.
[49] W. He, Y. Liu, J. Yuan, J.-J. Yin, X. Wu, X. Hu, K. Zhang, J. Liu, C. Chen, Y. Ji, Y. Guo, Au@Pt nanostructures as oxidase and peroxidase mimetics for use in immunoassays, Biomaterials 32 (4) (2011) 1139–1147.
[50] J. Liu, L. Meng, Z. Fei, P.J. Dyson, X. Jing, X. Liu, MnO_2 nanosheets as an artificial enzyme to mimic oxidase for rapid and sensitive detection of glutathione, Biosens. Bioelectron. 90 (2017) 69–74.
[51] T.B. Devi, D. Mohanta, M. Ahmaruzzaman, Biomass derived activated carbon loaded silver nanoparticles: an effective nanocomposites for enhanced solar photocatalysis and antimicrobial activities, J. Ind. Eng. Chem. 76 (2019) 160–172.
[52] D. Jiang, D. Ni, Z.T. Rosenkrans, P. Huang, X. Yan, W. Cai, Nanozyme: new horizons for responsive biomedical applications, Chem. Soc. Rev. 48 (14) (2019) 3683–3704.
[53] Y. Fang, Y. Zhang, L. Cao, J. Yang, M. Hu, Z. Pang, J. He, Portable Hg(2+) nanosensor with ppt level sensitivity using nanozyme as the recognition unit, enrichment carrier, and signal amplifier, ACS Appl. Mater. Interfaces 12 (10) (2020) 11761–11768.
[54] J. Zhu, X. Peng, W. Nie, Y. Wang, J. Gao, W. Wen, J.N. Selvaraj, X. Zhang, S. Wang, Hollow copper sulfide nanocubes as multifunctional nanozymes for colorimetric detection of dopamine and electrochemical detection of glucose, Biosens. Bioelectron. 141 (2019) 111450.
[55] J. Xi, J. Zhang, X. Qian, L. An, L. Fan, Using a visible light-triggered pH switch to activate nanozymes for antibacterial treatment, RSC Adv. 10 (2) (2020) 909–913.
[56] X. Niu, Y. He, J. Pan, X. Li, F. Qiu, Y. Yan, L. Shi, H. Zhao, M. Lan, Uncapped nanobranch-based CuS clews used as an efficient peroxidase mimic enable the visual detection of hydrogen peroxide and glucose with fast response, Anal. Chim. Acta 947 (2016) 42–49.
[57] P. Borthakur, P.K. Boruah, M.R. Das, Facile synthesis of CuS nanoparticles on two-dimensional nanosheets as efficient artificial nanozyme for detection of Ibuprofen in water, Chem. Eng. J. 9 (1) (2021) 104635.
[58] Z. Yang, S. Zhang, X. Zheng, Y. Fu, J. Zheng, Controllable synthesis of copper sulfide for nonenzymatic hydrazine sensing, Sensor. Actuator. B Chem. 255 (2018) 2643–2651.
[59] X. Xie, Z. Zhang, Y. Hu, H. Cheng, A mechanistic kinetic model for singlet oxygen mediated self-sensitized photo-oxidation of organic pollutants in water, Chem. Eng. J. 334 (2018) 1242–1251.
[60] J. Černý, M. Karásková, J. Rakušan, S. Nešpůrek, Reactive oxygen species produced by irradiation of some phthalocyanine derivatives, J. Photochem. Photobiol., A 210 (1) (2010) 82–88.
[61] R. Lavi, M. Sinyakov, A. Samuni, S. Shatz, H. Friedmann, A. Shainberg, H. Breitbart, R. Lubart, ESR detection of $^1O_2$ reveals enhanced redox activity in illuminated cell cultures, Free Radic. Res. 38 (9) (2009) 893–902.
[62] L.-Y. Jin, Y.-M. Dong, X.-M. Wu, G.-X. Cao, G.-L. Wang, Versatile and amplified biosensing through enzymatic cascade reaction by coupling alkaline phosphatase in situ generation of photoresponsive nanozyme, Anal. Chem. 87 (20) (2015) 10429–10436.